Journal of Medicinal Chemistry

Brief Article

Structure-Based Design of N-(3-((1H-pyrazolo[3, 4-b]pyridin-5-yl)ethynyl) Benzenesulfonamides as Selective Leucine-Zipper and Sterile-# Motif Kinase (ZAK) Inhibitors

Yu Chang, Xiaoyun Lu, Marthandam Asokan Shibu, Yi-Bo Dai, Jinfeng Luo, Yan Zhang, Yingjun Li, Peng Zhao, Zhang Zhang, Yong Xu, Zheng-Chao Tu, Qingwen Zhang, Cai-Hong Yun, Chih-Yang Huang, and Ke Ding

J. Med. Chem., **Just Accepted Manuscript** • Publication Date (Web): 06 Jun 2017

ACS Publications

Journal of Medicinal Chemistry is published by the American Chemical Society. 1155 Sixteenth Street N.W., Washington, DC 20036

Structure Based Design of *N*-(3-((1*H*-pyrazolo[3,4-*b*]pyridin-5-yl)ethynyl) Benzenesulfonamides as Selective Leucine-Zipper and Sterile-α Motif Kinase (ZAK) Inhibitors

Yu Chang,[#,†,‡] Xiaoyun Lu,[#,‡] Marthandam Asokan Shibu,[#,§] Yi-Bo Dai,[#,∥] Jinfeng Luo,[⊥] Yan Zhang,[⊥] Yingjun Li,[⊥] Peng Zhao,[∥] Zhang Zhang,[⊥] Yong Xu,[⊥] Zheng-Chao Tu,[⊥] Qing-Wen Zhang,[*,†] Cai-Hong Yun,[*,∥] Chih-Yang Huang,[*,§] and Ke Ding[*,‡]

[†]State Key Laboratory of Quality Research in Chinese Medicine, Institute of Chinese Medical Sciences, University of Macau, Macao, China

[‡]School of Pharmacy, Jinan University, 601 Huangpu Avenue West, Guangzhou 510632, China

[§]Graduate Institute of Basic Medical Science, China Medical University, Taichung, Taiwan; Department of Health and Nutrition Biotechnology, Asia University, Taichung, Taiwan, China

[∥] Institute of Systems Biomedicine, Department of Biophysics and Beijing Key Laboratory of Tumor Systems Biology, School of Basic Medical Sciences, Peking University Health Science Center, Beijing 100191, China

[⊥]Guangzhou Institutes of Biomedicine and Health, Chinese Academy of Sciences, 190 Kaiyuan Avenue, Guangzhou 510530, China

KEYWORDS: ZAK, myocardial hypertrophy, selective inhibitors

ABSTRACT: A series of *N*-(3-((1*H*-pyrazolo[3, 4-*b*]pyridin-5-yl)ethynyl)benzenesulfonamides were designed as the first class of highly selective ZAK inhibitors. The representative compound **3h** strongly inhibits the kinase activity of ZAK with an IC_{50} value of 3.3 nM, and dose-dependently suppresses the activation of ZAK downstream signals both *in vitro* and *in vivo*, while it is significantly less potent for the majority of 403 non-mutated kinases evaluated. Compound **3h** also exhibits orally therapeutic effects on cardiac hypertrophy in a spontaneous hypertensive rat model.

INTRODUCTION

Leucine-zipper and sterile-*α* motif kinase (ZAK) belongs to a mixed-lineage kinase family (MLKs), and structurally distinguishes itself from the other family members by presence of a sterile-*α* motif (SAM) domain. [1-4] ZAK is prominently expressed in heart (especially infarcted heart), skeletal muscle, placenta and liver etc. [2, 5, 6] Overexpression of ZAK has been closely related to the development of cardiac hypertrophy and myocardial fibrosis[7, 8] by activating downstream c-Jun *N*-terminal protein kinase (JNK) and p38 mitogen activated protein kinase (MAPK) pathways etc. [9-13] For instance, ZAK overexpression induced characteristic hypertrophic features in H9c2 cardio myoblast cells, including increasing cell sizes, expression of hypertrophic marker proteins (i.e. atrial natriuretic factor (ANF) and brain natriuretic peptide (BNP)), and actin fiber organization etc. [14-19] Conversely, cardio myoblast cells harboring dominant negative (DN) ZAK exhibited resistance against doxycycline induced hypertrophic feature transition and suppressed the expression of ANF and BNP. [15, 16] These data collectively suggest that ZAK may serve as a novel potential target to attenuate myocardial hypertrophy which is one of the most frequent causes of heart failure. [6]

There is no selective ZAK inhibitor reported to date, although a number of kinase inhibitors have been identified to exhibit unspecific suppression on the enzymatic function of ZAK. [7, 20-23] Given the fact that mechanisms of ZAK-induced myocardial hypertrophy remain elusive, it is highly desirable to discover selective small molecule ZAK inhibitors as research probes to further validate the physiological and/or pathological functions of ZAK in hypertrophic symptom development.

RESULTS AND DISCUSSION

ZAK shares an approximate 36% sequence identity with $Val^{600} \rightarrow Glu^{600}$ mutant of B-Raf serine/threonine protein kinase (B-Raf^{V600E}) that functions as a "driving force" for a variety of human cancers (e.g. melanoma, hairy cell leukemia and papillary thyroid carcinoma etc.) (Supporting Information, Figure S1). A superposition of the crystal structure of ZAK (PDB: 5HES)[20] with B-Raf^{V600E} (PDB: 4XV1) suggested that the hinge regions and *β*-sheets at *N*-lobes of the two proteins almost totally overlapped (Figure 2B). It is also noteworthy that several well characterized B-Raf^{V600E} inhibitors (e.g. vemurafenib (**1**)[20] and PLX4720 (**2**)[20, 24], Figure 1) display strong "off target" potencies against ZAK kinase. [7, 21, 25]

We recently discovered a series of *N*-(3-((1*H*-pyrazolo[3, 4-*b*]pyridin-5-yl)ethynyl)benzenesulfonamides as selective B-Raf^{V600E} inhibitors. [26] Although *N*-(3, 5-difluoro-4-((3-methoxy-1*H*-pyrazolo[3, 4-*b*]pyridin-5-yl)ethynyl)phenyl) benzenesulfona-mide (**3a**) exhibited moderate inhibitory

activity against B-Raf^{V600E} with an IC_{50} value of 169.2 nM, it potently suppressed ZAK with an IC_{50} value of 19.2 nM in an ADP-GloTM kinase assay. [27, 28] A preliminary computational study suggested that **3a** could fit nicely into the ATP binding site of ZAK and capture several key interactions with the protein. The 1*H*-pyrazolo[3, 4-*b*]pyridine moiety formed two hydrogen bonds with the backbone NH- and C=O of Ala85, respectively, in the hinge region, and it might also capture a potential π-π stacking interaction with Tyr84. The 2-ethynyl-1, 3-difluorophenyl linker could form a cation-π interaction with Lys45, while the sulfonamide group was crucial for the terminal phenyl group to adopt a backward-bending orientation and form a π-π interaction with Phe152 in the back pocket of the protein (Figure 2C). Investigation also implied that **3a** could bind with B-Raf^{V600E} with a similar mode to that of ZAK (supporting Information, Figure S2C).

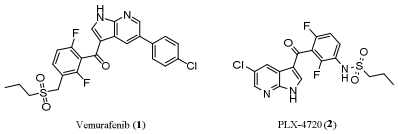

Figure 1. Chemical structures of non-selective ZAK inhibitors

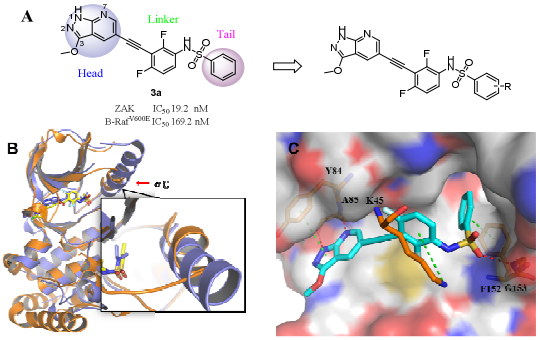

Figure 2. Design of selective ZAK inhibitors. (A) Molecular design of new ZAK inhibitors. (B) Superposition of ZAK (PDB: 5HES, orange) and B-Raf^{V600E} (PDB: 4XV1, purple). (C) Predicted binding model of **3a** (blue) with ZAK (PDB: 5HES, orange).

Scheme 1. Synthesis of Compounds 3a-3o.

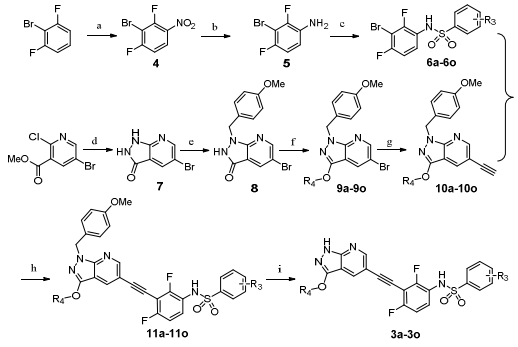

Reagents and conditions: (a) con. H_2SO_4, KNO_3, rt, 2 hrs, 91%; (b) $SnCl_2$, con. HCl, EtOH, reflux, 93%; (c) benzenesulfonyl chloride, pyridine, dry DCM, rt, 2 hrs, 93%; (d) $NH_2NH_2{\cdot}H_2O$, EtOH, 80 °C, overnight, 93%; (e) *p*-methoxybenzyl chloride, NaOH, DMSO, 0 °C to rt, 1 hr, 62%; (f) NaH, CH_3I, DMF, rt, overnight, 47%-53%; (g) (i) trimethylsilylacetylene, $Pd(dba)_2$, CuI, K_2CO_3, *t*-$(Bu)_3P$, THF, Ar_2, 120 °C, overnight, 51%; (ii) TBAF, THF, rt, 1 hr, 88% (two steps); (h) $Pd(dba)_2$, CuI, K_2CO_3, *t*-$(Bu)_3P$, THF, Ar_2, 120 °C, overnight, 50%; (i) TFA, reflux, overnight, 87%.

Table 1. *In Vitro* kinase inhibition of 3a-3o.

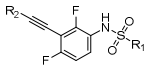

Cpds	R_1	R_2	Kinase inhibition (IC_{50} nM)		
			ZAK[a]	B-Raf^{V600E} [b]	B-Raf^{WT} [b]
3a			19.2±0.66	169.2±11.1	>10000
3b			5.1±0.31	>1000	>1000
3c			4.2±0.31	901.8±9.8	>6000
3d			16.8±0.40	>10000	>1000
3e			12.1±0.40	>10000	>10000
3f			7.5±0.65	>7000	>1000
3g			5.0±0.62	>1000	>1000
3h			3.3±0.29	>3000	>1000
3i			9.6±0.08	>10000	>2000
3j			22.6±0.86	>10000	>10000
3k			994.1±84.7	>10000	>10000
3l			5.1±0.63	>10000	>5000
3m			>30000	>10000	>10000
3n			42.7±4.2	>2000	>10000
3o			143.7±14.4	>10000	>10000
1	-	-	31.4±5.2 (23[c])	41.2±13.6	84.12± 27.8

[a]ZAK kinase inhibition was detected using ADP-Glo^{TM} kinase assay according to the manufacturer's instructions.[27,28] [b]Kinase inhibitions against B-Raf wild-type and V600E mutant were performed using FRET-based Z'-Lyte kinase assay according to the manufacturer's instructions as previously descripted.[26] The data are means from 3 independent experiments. [c]Reported data.[20,25]

ZAK possesses a slightly larger back pocket than B-Raf^{V600E} because of its outward shifting αC-helix (Figure 2B). A small hydrophobic substituent might be introduced at the terminal phenyl group in **3a** to improve the ZAK inhibitory potency and selectivity. Based on this hypothesis, compounds **3b**, **3c** and **3d**, in which a chloride was introduced at *ortho*-, *meta*- or

para- position of the corresponding phenyl moiety, respectively, were first designed and synthesized (Scheme 1). It was shown that *ortho*- (**3b**) and *meta*- (**3c**) substituted molecules indeed exhibited obviously improved ZAK inhibitory activities with IC_{50} values of 5.1 and 4.2 nM, respectively. The compounds also exhibited significantly increased target selectivity by abolishing the inhibition against B-Raf^{V600E}. Although a *para*-chloro substitution (**3d**) barely affected the ZAK suppressive function, it induced obvious improvement on ZAK selectivity. These data also suggested that *meta*- position of the phenyl ring is optimal for further optimization, and this position was well tolerated to a variety of substituents, such as methoxyl- (**3f**), bromo- (**3g**) and cyano- (**3h**) groups to exhibit strong and selective ZAK inhibitory potencies. For instance, compound **3h** strongly suppressed the kinase activity of ZAK with an IC_{50} value of 3.3 nM, but had no activity against wild-type B-Raf and its V600E variant. However, when the meta-chloride was replaced with a methyl group, the resulting compound 3**e** displayed a 3-folds potency loss. It was also noteworthy that the *ortho*-, *meta*- dichloride substituted derivative **3i** exhibited an IC_{50} value of 9.6 nM against ZAK, which is approximately 2 fold less potent than the corresponding mono-substituted compounds **3b** and **3c**.

The investigation further suggested the 3-methoxyl group in **3c** could be removed (**3l**) to display a similar potency and selectivity against ZAK with an IC_{50} value of 5.1 nM. However, the introduction of a large hydrophobic substituent, e.g. an iso-propoxyl (**3n**) or a cyclic-pentyloxyl (**3o**) group, caused approximately 10-34 folds potency loss. The corresponding compounds **3n** and **3o** exhibited IC_{50} values of 42.7 and 143.7 nM, respectively. Our modeling suggested that the potential dual hydrogen bond network between the 1*H*-pyrazolo[3, 4-*b*] pyridine moiety with Ala85 is critical for the binding of the compounds with ZAK protein. The replacement of the nitrogen atom (*N*) with a carbon at 7- position (**3k**) or methylation of the 1-NH moiety (**3m**) indeed resulted in almost total abolishment of ZAK inhibitory potency. The replacement of the 1*H*-pyrazolo[3, 4-*b*] pyridine moiety in **3l** with a 1*H*-pyrrolo[2, 3-*b*]pyridine group also caused a 5-fold potency loss. The resulting compound **3j** displaced an IC_{50} value of 22.6 nM against ZAK kinase.

Although the *meta*-substituted compounds **3c**, **3g**, **3h** and **3l** demonstrated the strongest ZAK inhibitory potencies, they failed to be docked into the ATP binding pocket of ZAK by utilizing the crystal structure previously disclosed (PDB: 5HES) because of a steric hindrance with Leu57. In order to elucidate detailed interaction between the inhibitors and ZAK, a 1.87 Å X-ray crystallographic structure of **3g**-ZAK complex was determined. In accordance with our prediction, the 1*H*-pyrazolo[3, 4-*b*]pyridine moiety indeed formed two critical hydrogen bonds and captured a π-π stacking interaction with Ala85 and Tyr84, respectively (Figure 3A). A cation-π interaction was also found between the difluorophenyl linker and Lys45. Additionally, two hydrogen bonds were formed between the sulfonamide and His158 and Gly153, respectively. Interestingly, the *meta*- bromine phenyl group in **3g** induced an outward rearrangement of the αC helix and a reorientation of Leu57 residue to avoid the potential steric hindrance with the molecule. The P-loop in the **3g**-ZAK complex crystal structure adopted a conformation dramatically different from that observed in the **1**-ZAK structure. This is likely because the P-loop in the **1**-ZAK complex was tethered by the hydrophobic interactions between the chlorobenzene moiety and Cys22/Phe27, while in **3g** the partially hydrophilic methoxyl moiety could not tether the P-loop in the same way.

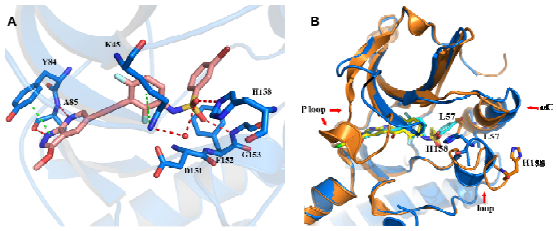

Figure 3. The co-crystal structure of inhibitor **3g** with ZAK. (A) Co-crystal structure of compound **3g** and ZAK. (PDB: 5X5O) (B) Superposition of previous ZAK (PDB: 5HES, orange) and **3g**-ZAK complex crystal structure (PDB: 5X5O, bule).

Taking **3h** as an example, its binding affinity with ZAK was further determined by using an active-site-dependent competition binding assay (conducted by Ambit Bioscience, San Diego, CA). It was shown that compound **3h** tightly bound to ZAK with a binding constant (K_d) value of 2.7 nM, but was obviously less potent for the majority of 468 kinases evaluated (including 403 nonmutated kinases and 65 mutated kinases). Its kinase selectivity S(10) and S(1)[30] scores are 0.017 and 0.002, respectively, at a concentration of 1.0 μM, which is approximately 370 fold higher than its K_d value with ZAK. The potential "off-target" kinases included aurora kinase B (AURKB), B-Raf^{V600E}, fyn-related kinase (FRK), KIT proto-oncogene receptor tyrosine kinase (KIT), mitogen extracellular-signal-regulated kinase kinase 5 (MEK5), salt-inducible kinase (SIK) and Src-related tyrosine kinase lacking C-terminal regulatory tyrosine and N-terminal myristylation sites (SRMS) etc. Further evaluation revealed that **3h** exhibited approximately 17-230-fold less potency against the majority of the "off target" kinases, with an exception of FRK, which displayed a K_d values of 22 nM (Figure 4B). These results collectively supported the extraordinary target specificity of **3h**.

Compound **3h** also exhibited reasonable pharmacokinetic properties in Spragur-Dawley (SD) rats, with an oral bioavailability of 20%, a high exposure value (areas under curve (AUC)) of 253794 μg/L·h and a $T_{1/2}$ value of 34.6 hrs at an oral dose of 10 mg/kg/day (Supporting Information, Table S5). Further determination revealed that the compound exhibited a hign plasma protein binding rate of 99.8% (Supporting Information, Table S6).

The potential therapeutic effect of **3h** on hypertrophy was first evaluated in an AngII induced myocardial hypertrophic cell model. Treatment of AngII obviously elevated the level of hypertrophic biomarker BNP and induced activation (phosphorylation) of JNK and P38 in H9c2 cardio myoblast cells. Whereas, compound **3h** dose-dependently suppressed elevation of the protein levels of BNP, phosphorylated JNK and phosphorylated p38, indicating its lockage on the AngII induced myocardial hypertrophy process (Figure 5).

The *in vivo* therapeutic efficacy of **3h** on myocardial hypertrophy was further investigated in spontaneous hypertensive rats (SHRs) which were previously validated to

harbor high level of ZAK kinase (Figure 6D). The normotensive Wistar-Kyoto (WKY) rats were utilized for direct comparison. The SHRs were randomly divided into 3 groups and treated with **3h** with oral dosages of 0, 10 or 20 mg/kg/day, respectively, for 4 continuous weeks based on PK profiles of the inhibitor. The experimental rats were sacrificed and the left ventricles were collected for biological determination. It was shown that the SHRs displayed greater left ventricular masse at diastole (LVd mass) and systole (LVs mass) than that of the normotensive WKY rats, indicating the hypertrophic symptom of the animals. Compound **3h** dose-dependently suppressed the LVd and LVs mass elevation in SHRs. For instance, the average LVd mass value was 1.20 grams for the vehicle control SHRs, while the values were decreased to 0.97 and 0.95 grams, which were close to the value in normotensive WKY rats, after 10.0 (SHR L) and 20.0 (SHR H) mg/kg/day treatments of **3h**, respectively (Figure 6A, 6B). The treatment also induced LVs mass decrease by 3.0-8.0%. Hematoxylin and eosin (H&E) biopsy staining images showed that the cardiomyocytes in normotensive control tissues displayed normal arrangement, whereas the tissue sections from SHRs exhibited more interstitial spaces (Figure 6C). Treatments of **3h** successfully restored the cardiomyocyte disarrangement to normal phenomena in a dose dependent manner. Consistent to the observation in H9c2 cells, compound **3h** also evidently interrupted the phosphorylation of JNK and p38 and decreased the level of BNP in the isolated left ventricles (Figure 6D). These data collectively demonstrated the therapeutic effect of **3h** on spontaneous hypertension-induced pathological cardiomyocyte hypertrophy.

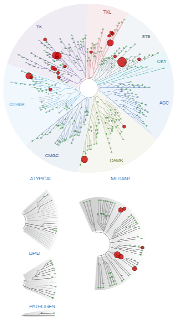

Kinases	%Ctrl@1000 nM	K_d (nM)[a]
ZAK	3	2.7
AURKB	2.4	64
BRAF(V600E)	9.9	60 (>10000[b])
FRK	1.9	22
KIT	6.2	460
KIT(L576P)	5.6	210
KIT(V559D)	2.9	180
MEK5	0.9	66
SIK	1.6	45
SRMS	3.9	64

[a] K_d values were calculated with a standard dose-response curve using the Hill equation. The data are the means from at least three independent experiments. [b] IC_{50} values were determinated using the FRET-based Z'-Lyte kinase assay according to the manufacturer's instructions. The data are means form at least two independent experiments.

Figure 4. KinomeScan kinase selectivity profiles of **3h**. (A) Compound **3h** was profiled at a concentration of 1.0 μM against a diverse panel of 468 kinases by DiscoveRx. (B) Binding constants (K_d values) of compound **3h** against the "top hits"

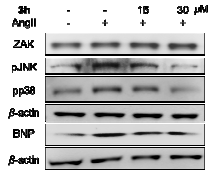

Figure 5. Compound **3h** dose-dependently inhibits the expression and phosphorylation of ZAK downstream signaling in AngII-induced H9c2 cardiomyoblast cells. The bands are representatives from 3 independent experiments.

CONCLUSION

In summary, a series of *N*-(3-((1*H*-pyrazolo[3, 4-*b*]pyridin-5-yl)ethynyl)benzenesulfonamides were discovered as novel selective ZAK inhibitors. One of the most promising compound **3h** strongly inhibits the kinase activity of ZAK with an IC_{50} value of 3.3 nM, and dose-dependently suppresses the activation of ZAK downstream signals both *in vitro* and *in vivo*. However, the compound is significantly less potent for a panel of 403 non-mutated kinases. A high resolution complex crystal structure was further determined to elucidate the detail interaction between an inhibitor and ZAK protein. Moreover, compound **3h** exhibits good pharmacokinetic properties and promising orally therapeutic effects on cardiac hypertrophy in a spontaneous hypertensive rat model. To the best of our knowledge, this molecule represents the first selective ZAK inhibitor demonstrating *in vivo* efficacy. The potent ZAK inhibitory activity and extraordinary target specificity make **3h** a valuable research probe for further biological investigation on ZAK.

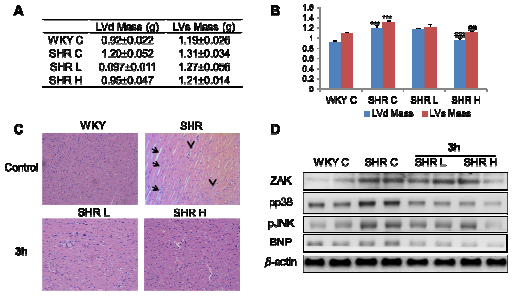

Figure 6. Compound **3h** inhibits myocardial hypertrophy *in vivo*. (A) Compound **3h** dose-dependently inhibits pathological increasing of left ventricular mass at diastole (LVd mass, bule) and systole (LVs mass, red). (B) Quantitative data for LVd and LVs masses. ***P<0.05 significant increase compared to WKY control rats. ##P<0.01, ###P<0.001 significant decrease compared to SHR rats (n = 6 per group). (C) Hematoxylin and eosin (H&E) staining images of the heart tissue sections. H&E-stained heart sections from normal rats treated with saline show normal architecture of cardiac myocytes with centrally placed nuclei. Heart sections from SHR rats show disorganization of the myofibrils with large inter spaces between the myocytes (long arrow) and abnormal nuclear orientation (arrow head). Treatment with **3h** ameliorate these effects noted in SHR rat hearts. (D) Compound **3h** dose-dependently inhibits the expression and phosphorylation of ZAK downstream signaling *in vivo*.

EXPERIMENTAL SECTION

General Chemistry. Reagents and solvents were obtained from commercial suppliers and used without further purification. Flash chromatography was performed using silica gel (200-300 mesh). All reactions were monitored by TLC, using silica gel plates with fluorescence F_{254} and UV light visualization. ^{1}H and ^{13}C NMR spectra were recorded on a Bruker AV-400 spectrometer at 400 MHz and Bruker AV-500 spectrometer at 125 MHz, respectively. Coupling constants (*J*) are expressed in hertz (Hz). Chemical shifts (δ) of NMR are reported in parts per million (ppm) units relative to internal control (TMS). The first-order peak patterns are indicated as *s* (singlet), *d* (doublet), *t* (triplet), *q* (quadruplet). Complex nonfirst-order signals are indicated as m (multiplet). The low- or high-resolution of ESI-MS was recorded on an Agilent 1200 HPLC-MSD mass spectrometer or Applied Biosystems Q-STAR Elite ESI-LC-MS/MS mass spectrometer, respectively. The purity of compounds was determined by reverse-phase high-performance liquid chromatography

(HPLC) analysis confirming to be over 95% (>95%). Analytical HPLC analyses were conducted using an Agilent 1260 system (G1310B Iso pump and G1365D MWD VL detector) with an YMC-Triart C_{18} reversed-phase column (250×4.6 mm, 5 μm) at 254 nm. Elution was MeOH in water and flow rate was 1.0 mL/min. Preparative HPLC (PHPLC) purifications were performed using Agilent 218 Solvent Delivery Module and an Agilent 325 dule wavelength UV-VIS detector with an YMC-Triart C_{18} reversed-phase column (250×20 mm, 5 μm) at 254 nm. The LC column was maintained at room temperature.

***In Vitro* Enzymatic Activity Assay.** The functional assays of compounds on the kinase activities of ZAK were determined using the ADP-Glo^{TM} kinase assay according to the manufacturer's instructions (Promega, Madison, WI).[27, 28] The reaction was carried out in a 384-well plate in a volume of 10 μL solvent containing 50 μM ATP, 200 μg/mL substrate (myelin basic protein, MBP) and serials of diluted compound with appropriate amount of kinase ZAK. Reactions were started immediately by adding ATP. After 30 min of incubation at room temperature, 10 μL of ADP-Glo reagent was added into each well to stop the reaction and consumed the remaining ADP within 40 min. At the end, 20 μL of kinase detection reagent was added into the well and incubated for 30 minutes to produce a luminescence signal and the light generated was examined with EnVision Multilabel Reader (Perkin Elmer, Inc.). Data analysis and curve fitting were performed using Graphpad Prism5 (Graphpad Software, Inc). Every experiment was repeated at least 3 times.

B-Raf, B-Raf^{V600E} (as B-Raf^{V600E} in supplier's catalogue) and the Z'-Lyte Kinase Assay Kit were purchased from Invitrogen. The experiments were performed according to the instructions of the manufacturer as previuosly descripted.[26] The concentrations of kinases were determined by optimization experiments and the respective concentration was: BRAF^{V600E} (PV4173, Invitrogen) 0.22 μg/μL. First, the compounds were diluted three-fold from 10^{-10} M to $1x10^{-4}$ M in DMSO and a 400 μM compound solution was prepared (4 μL compound dissolved in 96 μL water). Second, a 100 μM ATP solution in1.33×Kinase Buffer was prepared. Third, a kinase/peptide mixture containing 2×kinase and 4 μM Ser/Thr3 peptide (Invitrogen, PV3193) was prepared right before use. Kinase/peptide mixture was prepared by diluting Z'-LYTE Ser/Thr3 peptide (Invitrogen, PV3176) and kinase in 1×Kinase Buffer, and 0.2 μM Ser/Thr3 phospho-peptide solution was made by adding Z'-LYTE Ser/Thr3 phospho-peptide to 1×Kinase Buffer. The final 10 μL reaction consists of 0.002 ng of B-Raf, 2 μM Ser/Thr3 peptide in 1×kinase buffer. For each assay, 10 μL kinase reactions were made at first (including 2.5 μL compound solution, 5 μL Kinase/Peptide Mixture, and 2.5 μL ATP solution). Mixed the plate thoroughly and incubated for one hour at room temperature. Then 5 μL development solution was added to each well and the plate was incubated for 1h at room temperature; the nonphosphopeptides were cleaved at this time. In the end, 5 μL stop reagent was loaded to stop the reaction. For the control setting, 5 μL phospho-peptide solution instead of kinase-peptide mixture was used as 100% phosphorylation control. 2.5 μL 1.33×Kinase Buffer instead of ATP solution was used as 100% inhibition control, and 2.5 μL 4% DMSO instead of compound solution was used as the 0% inhibitor control. The plate was measured on an EnVision Multilabel Reader (Perkin-Elmer). Curve fitting and data presentations were performed using Graph Pad Prism, version 5.0. Every experiment was repeated at least for 3 times.

ASSOCIATED CONTENT

Supporting Information

Synthetic procedures and compound characterization, procedures, and *in vitro* enzymatic activity assay, amino acid sequence alignment, computational study, KINOME*scan*, animal expriments, western blot analysis, hematoxylin and eosin staining, crystallization and structure determination, pharmacokinetics study. ^{1}H NMR, ^{13}C NMR and HR MS spectra of compounds **3a-3o** (PDF) and Molecular Formula Strings (CSV).

AUTHOR INFORMATION

Corresponding Authors

*dingke@jnu.edu.cn (K. D.)
*cyhuang@mail.cmu.edu.tw (C.Y. H.)
*yunch@hsc.pku.edu.cn (C.H. Y.)
*qwzhang@umac.mo (Q.W. Z.)

Author Contributions

[#]Yu Chang, Xiaoyun Lu, Marthandam Asokan Shibu and Yi-Bo Dai contributed equally to this work.

Notes

The authors declare no competing financial interest.

ACKNOWLEDGMENT

The authors appreciate the financial support from National Natural Science Foundation of China (81425021, 81673285 and 31270769), Guangdong Province (2013A022100038, 2015A030312014, 2015A030306042, and 2016A050502041), Guangzhou City (201508030036), Jinan University and Taiwan Department of Health Clinical Trial and Research Center of Excellence (MOHW106-TDU-B-212-113004).

ABBREVIATIONS

ZAK, leucine-zipper and sterile-α motif kinase; MLK, mixed-lineage kinase; SAM, sterile-*α* motif; JNK, c-Jun *N*-terminal protein kinase; MAPK, mitogen activated protein kinase; ANF, atrial natriuretic factor; BNP, brain natriuretic peptide; DN, dominant negative; AURKB, aurora kinase B; FRK, fyn-related kinase; KIT, KIT proto-oncogene receptor tyrosine kinase; MEK5, mitogen extracellular-signal-regulated kinase kinase 5; SIK, salt-inducible kinase; SRMS, src-related tyrosine kinase lacking C-terminal regulatory tyrosine and *N*-terminal myristylation sites; SD, Spragur-Dawley; AUC, areas under curve; SHRs, spontaneous hypertensive rats; WKY, Wistar-Kyoto; LVd mass, left ventricular mass at diastole; LVs mass, left ventricular mass at systole; H&E, hematoxylin and eosin; SDS-PAGE, sodium dodecyl sulfate polyacrylamide gel electrophoresis; PVDF, polyvinylidene difluoride.

ANCILLARY INFORMATION

PDB code of ZAK-**3g** co-crystal structure: 5X5O.

REFERENCES

(1) Gallo, K. A.; Johnson, G. L. Mixed-lineage kinase control of JNK and p38 MAPK pathways. *Nat. Rev. Mol. Cell Bio.* **2002**, *3*, 663-672.

(2) Liu, T. C.; Huang, C. J.; Chu, Y. C.; Wei, C. C.; Chou, C. C.; Chou, M. Y. C.; Chou, K.; Yang, J. J. Cloning and expression of ZAK, a mixed lineage kinase-like protein containing a leucine-zipper and a sterile-alpha motif. *Biochem. Bioph. Res. Commun.* **2000**, *274*, 811-816.

(3) Gotoh, I.; Adachi, M.; Nishida, E. Identification and characterization of a novel MAP kinase kinase kinase, MLTK. *J. Biol. Chem.* **2001**, *276*, 4276-4286.

(4) Rana, A.; Rana, B.; Mishra, R.; Sondarva, G.; Rangasamy, V.; Das, S.; Viswakarma, N.; Kanthasamy, A. Mixed lineage kinase-c-Jun *N*-terminal kinase axis: a potential therapeutic target in cancer. *Genes Cancer* **2013**, *4*, 334-341.

(5) Abe, S.; Yagi, T.; Ishiyama, S.; Hiroe, M.; Marumo, F.; Ikawa, Y. Molecular cloning of a novel serine/threonine kinase, MRK, possibly involved in cardiac development. *Oncogene* **1995**, *11*, 2187-2195.

(6) Miyata, Y.; Akashi, M.; Nishida, E. Molecular cloning and characterization of a novel member of the MAP kinase superfamily. *Genes Cells* **1999**, *4*, 299-309.

(7) Manley, P. W.; Drueckes, P.; Fendrich, G.; Furet, P.; Liebetanz, J.; Baron, G. M.; Mestan, J.; Trappe, J.; Wartmann, M.; Fabbro, D. Extended kinase profile and properties of the protein kinase inhibitor nilotinib. *Biochim. Biophys. Acta* **2010**, *1804*, 445-453.

(8) Chang, Y.; Zhang, Q. W.; Li, Z. Q.; Ding, K.; Lu, X. Y. Leucine-zipper and sterile-α motif kinase (ZAK): a potential target for drug discovery. *Curr. Med. Chem.* **2016**, *23*, 3801-3812.

(9) Wong, J.; Smith, L. B.; Magun, E. A.; Engstrom, T.; Howard, K. K.; Jandhyala, D. M.; Thorpe, C. M.; Magun, B. E.; Wood, L. J. Small molecule kinase inhibitors block the ZAK-dependent inflammatory effects of doxorubicin. *Cancer Biol. Ther.* **2013**, *14*, 56-63.

(10) Stone, S. M.; Thorpe, C. M.; Ahluwalia, A.; Rogers, A. B.; Obata, F.; Vozenilek, A.; Kolling, G. L.; Kane, A. V.; Magun, B. E.; Jandhyala, D. M. Shiga toxin 2-induced intestinal pathology in infant rabbits is a-subunit dependent and responsive to the tyrosine kinase and potential ZAK inhibitor imatinib. *Front. Cell. Infect. Mi.* **2012**, *2*, 135-146.

(11) Eleanore, A. G.; Gallow, M. G.; Waldbaum, L.; Thomas, S.; Ruggieri, R. MRK, a mixed lineage kinase-related molecule that plays a role in γ-radiation-induced cell cycle arrest. *J. Biol. Chem.* **2002**, *277*, 13873-13882.

(12) Cheng, Y. C.; Kuo, W. W.; Wu, H. C.; Lai, T. Y.; Wu, C. H.; Hwang, J. M.; Wang, W. H.; Tsai, F. J.; Yang, J. J.; Huang, C. Y.; Chu, C. H. ZAK induces MMP-2 activity via JNK/p38 signals and reduces MMP-9 activity by increasing TIMP-1/2 expression in H9c2 cardiomyoblast cells. *Mol. Cell. Biochem.* **2009**, *325*, 69-77.

(13) Yang, J. J. Mixed lineage kinase ZAK utilizing MKK7 and not MKK4 to activate the c-Jun *N*-terminal kinase and playing a role in the cell arrest. *Biochem. Biophys. Res. Commun*. **2002**, *297*, 105-110.

(14) Huang, C. Y.; Chueh, P. J.; Tseng, C. T.; Liu, K. Y.; Tsai, H. Y.; Kuo, W. W.; Chou, M. Y.; Yang, J. J. ZAK re-programs atrial natriuretic factor expression and induces hypertrophic growth in H9c2 cardiomyoblast cells. *Biochem. Biophys. Res. Commun*. **2004**, *324*, 973-980.

(15) Hsieh, Y. L.; Tsai, Y. L.; Shibu, M. A.; Su, C. C.; Chung, L. C.; Pai, P.; Kuo, C. H.; Yeh, Y. L.; Viswanadha, V. P.; Huang, C. Y. ZAK induces cardiomyocyte hypertrophy and brain natriuretic peptide expression via p38/JNK signalling and GATA4/c-Jun transcriptional factor activation. *Mol. Cell. Biochem.* **2015**, *405*, 1-9.

(16) Huang, C. Y.; Kuo, W. W.; Chueh, P. J.; Tseng, C. T.; Chou, M. Y.; Yang, J. J. Transforming growth factor-β induces the expression of ANF and hypertrophic growth in cultured cardiomyoblast cells through ZAK. *Biophys. Res. Commun*. **2004**, *324*, 424-431.

(17) Sugden, P. H.; Clerk, A. Cellular mechanisms of cardiac hypertrophy. *J. Mol. Med.* **1998**, *76*, 725-746.

(18) Hanford, D. S.; Thuerauf, D. J.; Murray, S. F.; Glembotski, C. C. Brain natriuretic peptide is induced by α_1-adrenergic agonists as a primary response gene in cultured rat cardiac myocytes. *J. Biol. Chem.* **1994**, *269*, 26227-26233.

(19) Yamamoto, K.; Burnett, J. C.; Jougasaki, M.; Nishimura, R. A.; Bailey, K. R.; Saito, Y.; Nakao, K.; Redfield, M. M. Superiority of brain natriuretic peptide as a hormonal marker of ventricular systolic and diastolic dysfunction and ventricular hypertrophy. *Hypertension* **1996**, *28*, 988-994.

(20) Mathea, S.; Azeez, K. R. A.; Salah, E.; Tallant, C.; Wolfreys, F.; Konietzny, R.; Fischer, R.; Lou, H. J.; Brennan, P. E.; Schnapp, G.; Pautsch, A.; Kessler, B. M.; Turk, B. E.; Knapp, S. Structure of the human protein kinase ZAK in complex with vemurafenib. *ACS Chem. Biol.* **2016**, *11*, 1595-1602.

(21) Sauter, K. A. D.; Magun, E. A.; Iordanov, M. S.; Magun, B. E. ZAK is required for doxorubicin, a novel ribotoxic stressor, to induce SAPK activation and apoptosis in HaCaT cells. *Cancer Biol. Ther.* **2010**, *10*, 258-266.

(22) Vin, H.; Ojeda, S. S.; Chine, G.; Leung, M. L.; Chitsazzadeh, V.; Dwyer, D. W.; Adelmann, C. H.; Restrepo, M.; Richards, K. N.; Stewart, L. R.; Du, L.; Ferguson, S. B.; Chakravarti, D.; Ehrenreiter, K.; Baccarini, M.; Ruggieri, R.; Curry, J. L.; Kim, K. B.; Ciurea, A. M.; Duvic, M.; Prieto, V. G.; Ullrich, S. E.; Dalby, K. N.; Flores, E. R.; Tsai, K. Y. BRAF inhibitors suppress apoptosis through off-target inhibition of JNK signalling. *Elife* **2013**, *2*, e00969.

(23) Vin, H.; Ching, G.; Ojeda, S. S.; Adelmann, C. H.; Chitsazzadeh, V.; Dwyer, D. W.; Ma, H.; Ehrenreiter, K.; Baccarini, M.; Ruggieri, R.; Curry, J. L.; Ciurea, A. M.; Duvic, M.; Busaidy, N. L.; Tannir, N. M.; Tsai, K. Y. Sorafenib suppresses JNK-dependent apoptosis through inhibition of ZAK. *Mol. Cancer Ther.* **2014**, *13*, 221-229.

(24) Zhang, C.; Spevak, W.; Zhang, Y.; Burton, E. A.; Ma, Y.; Habets, G.; Zhang, J.; Lin, J.; Ewing, T.; Matusow, B.; Tsang, G.; Marimuthu, A.; Cho, H.; Wu, G.; Wang, W.; Fong, D.; Nguyen, H.; Shi, S.; Womack, P.; Nespi, M.; Shellooe, R.; Carias, H.; Powell, B.; Light, E.; Sanftner, L.; Walters, J.; Tsai, J.; West, B. L.; Visor, G.; Rezaei, H.; Lin, P. S.; Nolop, K.; Ibrahim, P. N.; Hirth, P.; Bollag, G. RAF inhibitors that evade paradoxical MAPK pathway activation. *Nature* **2015**, *526*, 583-586.

(25) Davis, M. I.; Hunt, J. P.; Herrgard, S.; Ciceri, P.; Wodicka, L. M.; Pallares, G.; Hocker, M.; Treiber, D. K.; Zarrinkar, P. P. Comprehensive analysis of kinase inhibitor selectivity. *Nat. Biotech.* **2011**, *29*, 1046-1051.

(26) Li, Y.; Cheng, H.; Zhang, Z.; Zhuang, X.; Luo, J.; Long, H.; Zhou, Y.; Xu, Y.; Taghipouran, R.; Li, D.; Patterson, A.; Smaill, J.; Tu, Z.; Wu, D.; Ren, X.; Ding, K. *N*-(3-ethynyl-2, 4-difluorophenyl) sulphonamide derivatives as selective Raf inhibitors. *ACS Med. Chem. Lett.* **2015**, *6*, 543-547.

(27) Auld, D. S.; Zhang, Y. Q.; Southall, N. T.; Rai, G.; Landsman, M.; Maclure, J.; Langevin, D.; Thomas, C. J.; Austin, C. P.; Inglese, J. A. A basis for reduced chemical library inhibition of firefly luciferase obtained from directed evolution. *J. Med. Chem.* **2009**, *52*, 1450-1458;

(28) Walsh, D. A.; Glass, D. B. Utilization of the inhibitor protein of adenosine cyclic monophosphate-dependent protein kinase, and peptides derived from it, as tools to study adenosine cyclic monophosphate-mediated cellular processes. *Method Enzymol.* **1991**, *201*, 304-316.

(29) Chinchilla, R.; Najera, C. The sonogashira reaction: a booming methodology in synthetic organic chemistry. *Chem. Rev.* **2007**, *107*, 874-922.

(30) Definition of S(10) and S(1): S(10)=(number of non-mutant kinases with %Ctrl <10)/(number of non-mutant kinases tested); S(1)=(number of non-mutant kinases with %Ctrl <1)/(number of non0mutant kinases tested).